Published in final edited form as:
Brain Res. 2012 December 3; 1487: 107–122. doi:10.1016/j.brainres.2012.05.064.

Evidence for connexin36 localization at hippocampal mossy fiber terminals suggesting mixed chemical/electrical transmission by granule cells

Dr. James I. Nagy
Department of Physiology, Faculty of Medicine, University of Manitoba, Winnipeg, Manitoba, Canada nagyji@ms.umanitoba.ca Tel. 204 789 3767, Fax 204 789 3934

Abstract

Electrical synaptic transmission via gap junctions has become an accepted feature of neuronal communication in the mammalian brain, and occurs often between dendrites of interneurons in major brain structures, including the hippocampus. Electrical and dye-coupling has also been reported to occur between pyramidal cells in the hippocampus, but ultrastructurally-identified gap junctions between these cells have so far eluded detection. Gap junctions can be formed by nerve terminals, where they contribute the electrical component of mixed chemical/electrical synaptic transmission, but mixed synapses have only rarely been described in mammalian CNS. Here, we used immunofluorescence localization of the major gap junction forming protein connexin36 to examine its possible association with hippocampal pyramidal cells. In addition to labelling associated with gap junctions between dendrites of parvalbumin-positive interneurons, a high density of fine, punctate immunolabelling for Cx36, non-overlapping with parvalbumin, was found in subregions of the stratum lucidum in the ventral hippocampus of rat brain. A high percentage of Cx36-positive puncta in the stratum lucidum was localized to mossy fiber terminals, as indicated by co-localization of Cx36-puncta with the mossy terminal marker vesicular glutamate transporter-1, as well as with other proteins that are highly concentrated in, and diagnostic markers of, these terminals. These results suggest that mossy fiber terminals abundantly form mixed chemical/electrical synapses with pyramidal cells, where they may serve as intermediaries for the reported electrical and dye-coupling between ensembles of these principal cells.

Keywords

granule cells; gap junctions; mixed electrical-chemical synapses; pyramidal cells

1. Introduction

Electrical synaptic transmission and the ultrastructural correlate of electrical synapses, consisting of connexin proteins that form intercellular channels at gap junctions between neurons, are now accepted features of neuronal circuitry in many areas of the mammalian central nervous system (CNS) (Bennett and Zukin, 2004; Hormuzdi et al., 2004; Connors and Long, 2004). Early ultrastructural, dye-coupling and electrophysiological studies

indicated the presence of electrical synapses in various areas of adult mammalian CNS (reviewed in Nagy and Dermietzel, 2000), but these synapses were generally considered to be rare and of little functional significance. Reports over the past decade, however, have revealed the prevalence and functional importance of electrical synapses in most major regions of mammalian CNS. This new understanding was aided by three factors: i) increased sophistication in electrophysiological approaches to recording from neurons, allowing application of stringent criteria for identification of electrical synapses (see Bennett, 2000); ii) discovery in 1998 of the first and most widely expressed connexin (Cx36) in neurons (Condorelli et al., 1998; Sohl et al., 1998), permitting detection of Cx36 in neurons and its immunohistochemical visualization in neuronal gap junction in widespread areas of mammalian CNS (Condorelli et al., 2000; Rash et al., 2000, 2001); and iii) development of Cx36 knockout mice, allowing demonstrations that Cx36 is required for formation of electrical synapses and for identification of CNS functional deficits in Cx36 knockout mice (Hormuzdi et al., 2004; Sohl et al., 2004).

In the hippocampus, gap junctions forming electrical synapses between various classes of interneurons are well-documented ultrastructurally and electrophysiologically (Kosaka, 1983a,b; Kosaka and Hama, 1985; Katsumaru et al., 1988; Ribak et al., 1993; Fukuda and Kosaka 2000; Zsiros and Maccaferri, 2005), and are considered to promote synchronous activity among these neurons, enabling synchronous high frequency γ-oscillations in pyramidal cells, which is disrupted in Cx36 knockout mice (Buhl et al., 2003; Maier et al., 2002). Because gap junction channels allow the intercellular passage of small molecules, including low molecular weight fluorescent dyes, early observations of cell-to-cell passage of dye (dye-coupling) between pyramidal cells in the hippocampus was taken as evidence that these cells are also linked with each other via electrical synapses (MacVicar and Dudek, 1981; Andrew et al., 1982; Dudek et al., 1983; Baimbridge et al., 1991; Church and Baimbridge, 1991). Subsequently, it was suggested that such synapses may occur between the axons of hippocampal pyramidal cells near their somata (Schmitz et al,. 2001). Recently, paired recordings from a large number of hippocampal pyramidal cells have provided further electrophysiological support for electrical coupling between these cells (Mercer et al., 2006; see also Bennett and Pereda, 2006).

A major difficulty in understanding potential functional contributions of electrical synapses between hippocampal pyramidal cells is the lack of ultrastructural identification of gap junctions associated with these neurons and, hence, uncertainty regarding the anatomical locations at which they may occur. Despite extensive analysis, the same thin-section transmission electron microscopic (TEM) studies that described many gap junctions between interneurons in the rat hippocampus revealed that similar large gap junctions did not occur between dendrites of pyramidal cells (Kosaka and Hama, 1985). It is possible, however, that gap junctions between these cells may be too small to detect in conventional thin-section images (Rash et al., 1998). Moreover, freeze-fracture images of gap junctions reported on putative CA3 pyramidal cells (Schmalbruch and Jahnsen, 1981) appear to have been misidentified glial junctions, based on the presence of oligodendrocyte membrane markers (large IMP-free areas and “reciprocal patches”) (Rash et al., 1998). Further, electrical synapses can occur between various neuronal elements, e.g., axo-axonic, dendro-dendritic, somato-somatic, axo-somatic. Given the high magnifications required to visualize small gap junctions by TEM, and consequent limitations in dimensions of tissues that can be analyzed, ultrastructural detection of electrical synapses depends crucially on the cellular and subcellular structures under examination. With this consideration in mind, several very small gap junctions were recently found linking mossy fiber axons in rat hippocampus (Hamzei-Sichani et al., 2007).

When gap junctions are present at nerve terminals, both chemical and electrical transmission may occur at what are termed mixed synapses. The functional importance of neuronal gap junctions at such chemical/electrical mixed synapses has been extensively documented in lower vertebrates, among the most classic of which are the large Club Ending terminals on Mauthner cells in teleost brain (Pereda et al., 2003, 2004). Mixed synapses have been described in the lateral vestibular nucleus and spinal cord of rat (Korn et al., 1973; Rash et al., 1996), but have been considered to be rare or absent in most other regions of mammalian CNS. Early and more recent reports of dye and electrical coupling between hippocampal pyramidal cells prompted the present re-examination of Cx36 localization in the hippocampus, with a focus on sites where it might exhibit close association with pyramidal cells. Using immunofluorescence detection of Cx36 in combination with various marker proteins that are highly concentrated in mossy fiber terminals, including vesicular glutamate transporter-1 (vglut-1), bassoon, AF6 and zonula occludens-1 (ZO-1), we present evidence for Cx36 localization at these terminals, suggesting that mossy fiber terminals form glutamatergic mixed synapses with hippocampal pyramidal cells.

2. Results

2.1. Immunofluorescence localization of Cx36 in the hippocampus

As elsewhere in the rat CNS, immunolabelling for Cx36 in the hippocampus was typically punctate, with these puncta presumably corresponding to sites of Cx36-containing interneuronal gap junction plaques that have been described ultrastructurally by freeze-fracture replica immunogold labelling (FRIL) for Cx36 in small plaques elsewhere in rodent brain (Rash et al., 2001,2004,2007a,b; Kamasawa et al., 2006). Intracellular immunolabelling with the set of antibodies against Cx36 used here was not evident, thus precluding identification of Cx36-expressing cells by detection of label within neuronal somata. However, neuronal gap junctions composed of Cx36 in the hippocampus often occur between interneurons containing parvalbumin (PV) (Kosaka and Hama, 1985; Katsumaru et al., 1988; Ribak et al., 1993; Fukuda and Kosaka, 2000; Meyer et al., 2002; Baude et al., 2007). Thus, to search for potential anatomical relationships between Cx36 and hippocampal pyramidal cells, rat hippocampal sections were double-labelled for PV and Cx36 to determine the extent to which Cx36-puncta can be accounted for by their association with PV-positive processes. Along the septo-temporal axis of the hippocampus, PV-positive interneurons with cell bodies located in the pyramidal cell layer (PCL) extend dendrites into the stratum oriens and the stratum radiatum. As expected and here presented as a positive control for PV/Cx36 co-localization, linear arrays of Cx36-immunopositive puncta within these strata were readily found along PV-immunoreactive dendrites, as shown in the stratum radiatum of the ventral hippocampal CA1 area (Fig. 1A).

Interneurons containing PV are also distributed in the CA3 area, and some of these have somata dispersed in the PCL, with dendrites percolating through the stratum lucidum (SL) (Fig. 1B1). As elsewhere in the hippocampus, immunofluorescence labelling for Cx36 in the SL consisted of sparsely distributed, relatively large Cx36-positive puncta (Fig. 1B2), many of which were localized to PV-positive dendrites, including points where branches of different dendrites intersected, presumably forming gap junctions (Fig. 1B3). In addition to these large puncta, and unlike corresponding regions of the CA3 subfield in the dorsal hippocampus, the CA3b subfield and distal portions of the CA3c subfield in the ventral hippocampus contained hitherto undescribed very fine, abundant Cx36-positive puncta that were restricted to the confines of the SL and partly extended into the PCL (Fig. 1B2). These fine Cx36-puncta displayed negligible co-localization with PV-positive processes within the SL (Fig. 1B3). As a control for specificity of immunofluorescence detection of these Cx36-puncta, two anti-Cx36 antibodies generated against different non-overlapping peptide sequences in Cx36 were used. Results with anti-Cx36 Ab39-4200 are shown in (Fig. 1B).

Similar fine, punctate labelling in the SL of ventral hippocampal CA3b was obtained with Ab37-4600, and this labelling also showed minimal co-localization with PV-positive processes (Fig. 1C). A further control involved double-labelling with monoclonal anti-Cx36 Ab39-4200 and polyclonal Ab37-4600, which examined by confocal analysis established that these antibodies produce labelling of the same identical puncta (Fig. 1D). This provides confidence in Cx36 detection at gap junctions because it is unlikely that the two anti-Cx36 antibodies cross react with proteins sharing a common subcellular site as small as a gap junction.

2.2. Immunofluorescence of Cx36 and markers of mossy fiber terminals

With the high density of fine Cx36-puncta observed in the SL, we examined possible association of these puncta with mossy fiber terminals. The SL represents the location of these terminals, which originate from axonal projections of granule cells in the dentate gyrus. Various proteins are highly concentrated in mossy terminals, and have been used as immunocytochemical markers for these terminals. Four such markers employed here alone and in combination, included: vglut-1, associated with synaptic vesicles in mossy terminals (Kaneko et al., 2002; Hagiwara et al., 2005; Jaffe and Gutierrez, 2007); bassoon, concentrated at numerous and relatively large active zones of mossy terminal synapses (tom Dieck et al., 1998; Hagiwara et al. 2005), but occur at other synapses as well (Richter et al, 1999), and in the SL may therefore not be localized exclusively to mossy terminals; and AF6 and ZO-1, associated with puncta adhaerentia type junctions between mossy fiber terminals and pyramidal cell dendrites (Inagari et al., 2003; Nishioka et al., 2000). Puncta adhaerentia typically occur at large synapses, and are a hallmark of mossy fiber terminals, where they occur at contacts between these terminals and exclusively the dendritic shafts of pyramidal cells (Amaral and Dent, 1981; Rollenhagen and Jubke, 2006; Rollenhagen and Lubke, 2010). To our knowledge, they have not been described between other neuronal elements in the SL. Although ZO-1 is also localized to tight junctions, such junctions do not occur between mossy terminals (Inagari et al., 2003), but instead, ZO-1 is commonly localized to Cx36-containing neuronal gap junctions, as we have described elsewhere in brain (Li et a., 2004). In sections cut perpendicular to the septo-temporal axis at various hippocampal levels, immunofluorescence labelling intensity for each of these proteins was much greater in the SL than in surrounding areas in the hippocampus, thus clearly delineating the SL (Fig. 2A-D). Reference to the proximal-distal regions of the CA3 subfields as CA3c, CA3b and CA3a, shown in Fig. 2A, is according to previously described hippocampal nomenclature (Scharman, 1993; Ishizuka et al., 1995).

Laser scanning confocal double-immunofluorescence imaging for these proteins in combination with Cx36 was examined in the ventral hippocampus at the rostro-caudal plane shown in a section immunostained for vglut-1 (Fig 2E), corresponding roughly to transverse level of Bregma minus 5.2 in the rat brain atlas of Paxinos and Watson (Paxinos and Watson, 1986). The appearance of fine Cx36-puncta in the SL at this level is shown in an extended photomontage encompassing a 1.7 mm length along the SL, where labelling for Cx36 is seen straddling each side of the PCL and occurs sparsely within the PCL (Fig. 2F). In sections double-labelled for vglut-1 and Cx36, punctate labelling for Cx36 was co-distributed with labelling for vglut-1 in the SL (Fig. 3A), where vglut-1 is reported to be exclusively in mossy fiber terminals (Kaneko et al., 2002; Jaffe and Gutierrez, 2007). Some Cx36-puncta/vglut-1 co-localization was also seen at the basal areas of the PCL, where some mossy fiber terminals are known to occur in the proximal regions of CA3 (Witter and Amaral, 2004). Higher magnification immunofluorescence analysis of z-stack images revealed that the majority of Cx36-puncta in the SL overlap with mossy terminals labelled for vglut-1 (Fig. 3B). Commonly observed were clusters of four to eight Cx36-puncta that were co-localized with individual but much larger vglut-1-positive terminals (Fig. 3B, inset).

Similar co-localization was also seen after double-labelling for bassoon combined with Cx36 (Fig. 3D).

Three image manipulations were undertaken as controls to establish that overlap of labelling for vglut-1 with Cx36 was not simply coincidental, arising from the high concentration of labelling for each marker in the SL, nor was it due to apparent overlap of Cx36-puncta and vglut-1-labelled mossy terminals that were actually separated in the vertical dimension in z-stack images. First, a 180° horizontal flip of the vglut-1 z-stack image in Figure 3B1, as shown in Figure 3C1, followed by overlay with labelling for Cx36 in the same field, gave minimal vglut-1/Cx36 co-localization (Fig. 3C3), indicating the observed co-localization in Fig. 3B1 is not simply a random occurrence. Second, single scan confocal images showed the same degree of Cx36 overlap with vglut-1 in mossy terminals as seen in z-stack images (supplementary Fig. 1A). And third, rotating the entire z-stack overlay image in Figure 3B3 along the y-axis showed that the vast majority of vglut-1/Cx36 association was maintained during rotation (supplementary Fig. 2, movie), further indicating that this association was not an artifact of z-stack imaging.

Immunofluorescence labelling of Cx36 in combination with AF6 and with ZO-1, as well as triple immunolabelling of Cx36 in combination with vglut-1 and AF6, in the region of the boxed area indicated in Figure 2E is shown in Figure 4, and Fig. 5A and B. Similar to results obtained with vglut-1, immunolabelling for AF6 and ZO-1 in mossy fiber terminals was co-distributed with Cx36-positive puncta in the SL, and co-localization of these two markers with Cx36 was evident even at relatively low magnification (Fig. 4A and 5A). Laser scanning confocal z-stack images indicated that nearly all Cx36-puncta in the SL overlapped with labelling for AF6 (Fig. 4B), and that the vast majority of Cx36-puncta also overlapped with labelling for ZO-1 (Fig. 5B). Again, as with vglut-1, a 180° horizontal flip of the AF6 z-stack image in Figure 4B1, yielding the image in Figure 4C1, followed by overlay with labelling for Cx36 in the same field, gave minimal AF6/Cx36 co-localization (Fig. 4C3). Likewise, minimal artifactual co-localization was observed following rotation and overlay of the ZO-1/Cx36 images (not shown). Further, rotating the z-stack AF6/Cx36 overlay image in Figure 4B3 along the y-axis maintained AF6/Cx36 co-localization during rotation (supplementary Fig. 3, movie).

Relationships between vglut-1-positive mossy terminals, AF6 and Cx36-puncta were more evident in triple labelled sections (Fig. 4D). Immunofluorescence for AF6 was seen to occupy subregions of vglut-1 labelled terminals, as might be expected based on the reported high concentration of AF6 at adhaerentia-like junctions formed at the plasma membrane of mossy terminals and absence of labelling for AF6 elsewhere within these terminals (Nishioka et al., 2000). Labelling for Cx36 was, in turn, often localized to small portions of AF6-positive patches, with Cx36-puncta usually occurring at the edges of these patches (Fig. 4D), suggesting close association of Cx36-containing gap junctions to adhaerentia-like junctions.

The distribution of Cx36-puncta in the SL was further examined in relation to N-methyl-D-aspartate receptor subunit NR1, which is known to be a component at mossy terminals, although it is more sparsely expressed in the SL compared with other regions of the hippocampus (Siegel et al., 1994; Watanabe et al., 1998; Jaffe and Gutierrez, 2007). In sections triple labelled for vglut-1, NR1 and Cx36 (Fig. 6), labelling for NR1 was exclusively punctate in appearance and largely overlapped labelling for vglut-1. Cx36-puncta were often seen interspersed among collections of NR1-positive puncta at sites of vglut-1-positive terminals, consistent with the localization of Cx36 at or near structures involved in glutamatergic neurotransmission.

2.3. Quantitative analysis of Cx36 puncta in the SL

Quantification was undertaken to determine the extent to which Cx36-puncta were co-localized with mossy fiber terminals immunolabelled for vglut-1 in the SL of the ventral hippocampal CA3b region. Counts of Cx36-positive puncta in confocal images were conducted using tissue from two rats. Localization relationships between Cx36-positive puncta and labelling for vglut-1 were categorized as: a) totally overlapping; b) as in apposition where Cx36-puncta were immediately adjacent to vglut-1-positive terminals; or c) as totally separate (i.e., > 0.5 m). Analysis of a total of 1,910 Cx36-puncta in 28 randomly selected fields in the SL of one rat gave 74 ± 1.9% (mean ± s.e.m.) Cx36/vglut-1 co-localization, 15 ± 1.4% adjacent, and 11 ± 1.1% separate. Analysis of a total of 1,505 puncta in 26 fields of the SL in the second rat gave 78 ± 1.9% Cx36/vglut-1 co-localization, 12 ± 1.3% adjacent, and 10 ± 1.4% separate.

The above results suggest the presence of Cx36-containing gap junctions between mossy fiber terminals and hippocampal pyramidal cells, or possibly between mossy fiber terminals themselves. As a means to correlate potential functional significance of gap junctions in the SL of the CA3b region in adult rat hippocampus with that in a neuronal network where electrical coupling is well established, namely the inferior olivary nucleus, we compared the relative density of Cx36-puncata in the SL of CA3b rat ventral hippocampus vs. inferior olive by counting the number of small to large Cx36-puncta in defined tissue volumes, according to our previous methods (Li et al., 2008). Quantitative analysis of the density of Cx36-puncta in the SL revealed that a volume of 80 × 80 × 3.6 μm (23,040 μm^3) within this field contained 122 ± 5.7 puncta (mean ± s.e.m.), compared with a value of 308 ± 4 Cx36-puncta in a similar volume of the inferior olivary nucleus. Examples of images used for counts of Cx36-puncta in the SL and the inferior olive are shown in Fig. 5C and 5D, respectively. The total area occupied by the subportion of the SL containing abundant Cx36, as determined in sections cut perpendicular to the extended septo-temporal axis of the hippocampus and double-labelled for Cx36 and bassoon, was found to be 141,763 ± 10,596 μm^2 (mean ± s.e.m.). From these values, we calculated that the volume occupying the portion of the SL containing Cx36-puncta over a length of 25 μm along this axis (a value chosen as a relatively readily identifiable measure corresponding to the average diameter of a pyramidal cell) was 3,544,075 μm^3 (25 μm × 141,763 μm^2), and that this volume contained 18,750 Cx36-positive puncta. Similar analysis of the density of Cx36- puncta in an equal volume of neuropil in the inferior olivary nucleus, where critical functions of electrical synapses containing Cx36 have been well documented (Hormuzdi *et al.*, 2004), was determined to be 47,380 Cx36-positive puncta, which is only 2.5-fold greater than that in the ventral hippocampal SL of CA3b (i.e., the ventral SL has 40% of the density of Cx36 puncta as in the inferior olive).

2.4. Regional and species differences in hippocampal Cx36

Compared with dense punctate labelling for Cx36 in the rat ventral hippocampal CA3b and distal portions of the CA3c hippocampal subregions described above, the density Cx36-puncta ranged from very sparse to a near absence in the SL of the rat dorsal hippocampal CA3b region (Fig. 7A), to a near absence in the SL of the rat dorsal (Fig. 7B) and ventral (Fig. 7C) hippocampal CA3a region. Hippocampal areas shown in the images of Fig. 7A and 7B are represented by the lower and upper boxed areas shown in Fig. 2A. Thus, the portion of the SL containing Cx36 encompassed areas CA3b and the distal portion of CA3c of the ventral half of the hippocampal CA3 region along the dorsal-ventral axis. Surprisingly, the SL in the ventral hippocampal CA3b region in mouse brain, corresponding to that in rat hippocampus which contains abundant fine Cx36-puncta, was also nearly devoid of punctate labelling for Cx36 (Fig. 7D), as were all other regions of SL in mouse hippocampus. However, Cx36-puncta in other hippocampal regions of mouse were readily detectable,

including the CA3 hilar region shown as a positive control (Fig. 7E), with absence of these puncta in Cx36 knockout mice shown as a negative control (Fig. 7F).

3. Discussion

Based on immunofluorescence detection of punctate labelling for Cx36 co-localized with markers of mossy fiber terminals in the hippocampal SL of rat, the present results suggest that these mossy fiber terminals form gap junctions with their postsynaptic targets, thereby establishing mixed chemical/electrical synapses. In the absence of prior documentation of an electrical component at these synapses, and despite tremendous investigative efforts that have been focused on the hippocampus and specifically on transmission at mossy fiber terminals over the past decades, our findings may seem surprising, and will raise many questions. Certainly, our proposal of mixed synaptic transmission at mossy fiber terminals will require confirmation by ultrastructural visualization of gap junctions at these synapses and electrophysiological demonstration of their electrical component.

3.1. Cx36 co-localization with mossy fiber terminal markers

A small proportion of mostly larger Cx36-puncta in the SL were associated with interneurons that had PV-positive processes in the SL. Among the remaining fine Cx36-puncta, about 75% of these showed absence of overlap with PV-positive processes and total overlap with labelling for vglut-1. These results presumably reflect Cx36 association specifically with mossy terminals, because vglut-1 in the SL appears to be localized exclusively within this class of terminals (Kaneko et al., 2002; Jaffe and Gutierrez, 2007), and because mossy fiber pre-terminal axons do not contain high levels of vesicles, and therefore do not exhibit robust labelling for vglut-1. Mossy fiber terminals are typically 3-6 μm in diameter, while most Cx36-containing gap junctions are usually <0.2 μm (as determined by FRIL in ten gap junctions at unidentified nerve terminals in adult rat SL (Nagy and Rash, work in progress). However, some gap junctions appear slightly larger after immunofluorescence labelling, possibly due to halation (i.e., divergence of photons from a source). This, together with the lack of intracellularly detectable Cx36, gave rise to localization of Cx36-puncta in subportions of the total area of individual mossy terminals. The frequency with which these puncta occurred in closely arranged clusters suggests that individual mossy terminals form multiple gap junctions.

The above value of 75% for Cx36-puncta association with mossy terminals labelled for vglut-1 is almost certainly an underestimate for three reasons. First, situations in confocal images may be expected where Cx36/mossy terminal associations were captured, not en face and visualized as total overlap, but rather on edge. Thus, 12-15% of Cx36-puncta that were counted as being in apposition to labelling for vglut-1 may also represent co-localization with mossy fiber terminals. Second, because counts were conducted using single confocal scans, some Cx36-puncta designated as being separate from labelling for vglut-1 could be associated with mossy terminals out-of-field in the z-axis, as was evident in tests of this possibility by examination of adjacent images in z-stacks (data not shown). And third, while synaptic vesicles labelled for vglut-1 are widely distributed in mossy terminals, they do not occupy all of the territory in a terminal, and do not accumulate everywhere near the terminal plasma membrane (Rollenhagen and Lubke, 2010), which would be the subcellular site for gap junctions. Thus, Cx36-puncta seen only in apposition to mossy terminals, rather than overlapping with terminals, may represent cases where the entire intracellular compartment of these terminals, up to areas near the terminal plasma membrane, were not labelled for vglut-1. With these considerations, the degree of Cx36/mossy terminal association in the SL may well reach 90%. Although association of Cx36-puncta with several other markers of mossy terminals examined was not assessed quantitatively, visual inspection, particularly of labelling for Cx36 with AF6 and ZO-1, suggests a similarly high percentage of co-

localization. Overlap of Cx36-puncta with labelling for AF6 and ZO-1 is consistent with Cx36 localization to mossy fiber terminals that have high levels of these two proteins along their plasma membranes (Inagari et al., 2003; Nishioka et al., 2000). Moreover, our results also suggest direct molecular interaction of Cx36 with ZO-1 in these terminals, as we have shown in gap junctions elsewhere in brain (Li et al., 2004), as well as Cx36 interaction with AF6, as we have more recently reported (Li et al., 2011). Thus, ZO-1 and AF6 appear to associate not only with adherens junctions (Inagari et al., 2003; Nishioka et al., 2000), but possibly also with gap junctions in mossy terminals, as seen in other brain areas.

Neurons at early postnatal ages are reported to be extensively coupled by gap junctions (Fulton, 1995; Montoro and Yuste, 2004). Because granule cells are continually produced in adult dentate gyrus (Cameron and McKay, 2001), it might be proposed that Cx36-containing gap junctions in the SL of adult rats are associated primarily with terminals of newly generated granule cells, reflecting a process simply related to normal development. Notwithstanding that this would still invoke a novel feature involving mixed synapses, it seems unlikely that the relatively abundant Cx36-puncta observed in the SL are localized exclusively to mossy terminals arising from a relatively small number of newly generated granule cells. Moreover, our data and calculations indicate that the density of Cx36-puncta in SL is within the range of that seen in other regions of adult brain, such as the inferior olive, where Cx36-containing gap junctions are known to support physiologically important functions (Bennett and Zukin, 2004). Further, we have found far lower levels of Cx36-puncta in the SL at postnatal day six than in adult SL (not shown), which would not be expected if Cx36 in mossy fibers terminals was related exclusively to developmental events, although this requires a more comprehensive study of Cx36 in developing hippocampus.

3.2. Species differences contrasting Cx36 localization in the stratum lucidum

Our immunofluorescence studies of the distribution of Cx36 throughout mouse vs. rat brain and spinal cord (Nagy, unpublished observations) have so far revealed very few species differences. In curiously stark contrast is the major difference presently found in the hippocampus, where the entire SL of both dorsal and ventral hippocampus of *mouse* contains very little immunolabelling for Cx36 with both anti-Cx36 antibodies employed, despite these antibodies giving extensive positive immunolabelling for Cx36 associated with hippocampal interneurons in mouse. If Cx36-containing mossy fiber terminals form gap junction with pyramidal cells, which would then also be required to coordinately express Cx36, then the presently observed rat vs. mouse differences are consistent with earlier observations that hippocampal pyramidal neurons express Cx36 mRNA in rat (Belluardo et al., 2000; Condorelli et al., 2000), but not in mouse (Hormuzdi et al., 2001; Degen et al., 2004). The latter reports involving detection of Cx36 mRNA and lacZ reporter gene expression in mouse, also point to species-specific differences in Cx36 expression. These species-specific differences of uncertain origin appear to preclude the use of wild-type vs. Cx36 knockout mice for comparison and confirmation of electrical coupling at presumptive mixed chemical/electrical synapses between mossy fiber terminals and hippocampal pyramidal cells, but which will be possible with the development of Cx36 knockout rats.

It may be considered that, although the potentially complex process of mixed synaptic transmission at mossy fiber terminals may occur in rat hippocampus, the absence of such a process in mouse hippocampus raises serious questions as to its functional importance or requirement for optimal or enhanced network performance in rat. Evolutionarily, the *Mus* lineage diverged from the *Rattus* lineage about ten million years ago, providing ample opportunity for divergence of neural systems that orchestrate behavior. In comparisons of rats vs. mice in experimental paradigms designed to assess behavior, mice are generally found to exhibit simpler behavioral repertoires, slower leaning performance, and lower adaptive flexibility than rats, leading to the suggestion that mice have a more restricted

range of behavioral capacities than rats (Whishaw et al., 2001). These differences, of course, could be due to myriad factors. Nevertheless, given the importance of hippocampal functions in some of the key behavioral features in which mice and rats differ, it may be worth considering observed difference in the hippocampus as contributing to these factors.

3.3. Sub-regional differences in Cx36 localization in the stratum lucidum

The differential density of Cx36-puncta in the SL of the ventral vs. dorsal hippocampus implies differential expression of Cx36 in granule cell projecting to these regions, and adds to other differences that have been described in dorsal vs. ventral hippocampus (Papatheodoropoulos and Kostopoulos, 2000, 2002a,b; Papatheodoropoulos et al., 2002, 2005; Sotiriou et al., 2005). Pertinent in this regard are implications of abnormal neuronal gap junctional coupling in initiation, maintenance, and spread of epileptic activity and in hypersynchronous activity associated with seizures (Perez et al., 2000; Pike et al., 2000; Rouach et al., 2002; Traub et al., 2001). In hippocampus, our finding of Cx36 association with mossy terminals in the rat ventral CA3 region, where it presumably forms an abundance of chemical/electrical mixed synapses, and an absence of these in the dorsal region, may be considered in relation to reports that the ventral hippocampus is more excitable and shows greater epileptogenicity than its dorsal counterpart (Racine et al., 1977; Bragdon et al., 1986; Gilbert et al., 1985; Lee et al., 1990). Further, the CA3 region is more excitable than other hippocampal regions including the CA1 and dentate gyrus, generates intrinsic oscillatory frequencies (Pike et al., 2000; Buzsaki, 2002; Csicsvari et al., 2000, 2003; Traub et al., 1996), and plays a crucial role in the generation and propagation of seizures (Traub et al., 1996; 2001; Derchansky et al., 2006). While it is uncertain how malfunction of electrical synapses may contribute to seizure generation, genetic studies have indicated a link between mutations in Cx36 and juvenile myoclonic epilepsy, which is a common form of idiopathic generalized epilepsy (Mas et al., 2004; Hempelmann et al., 2006). The presence of Cx36-containing gap junctions adds to the possibility that electrical synapses formed by mossy fibers in the ventral hippocampus, and their potential malfunction, are among the dorsal-ventral differences contributing to the greater propensity for seizure generation in this region.

3.4. Functional considerations

The physiological impact of the electrical component of mossy fiber synapses on hippocampal network properties remains to be investigated. However, mossy terminals form synapses not only with pyramidal cells, but also with interneurons having dendrites in the SL (Acsady et al., 1998; Witter and Amaral, 2004). The average number of CA3 pyramidal cells contacted by the en passant nature of mossy fiber terminations is about 14, and each CA3 pyramidal cell receives inputs from on average 50 independent mossy fiber axons (Claiborne et al., 1986; Chicurel and Harris, 1992; Acsady et al., 1998; Witter and Amaral, 2004). Thus, assuming an even distribution of Cx36-containing gap junctions among mossy fiber terminals regardless of their targets, a single mossy fiber axon may establish electrical contacts with dendrites of several pyramidal cells, thereby providing a route for electrical coupling between pyramidal cells via intermediary mossy fibers. In this way, mossy fibers could establish assemblies of coupled cells based on those with which they form en passant synapses, as illustrated in Figure 8. It is interesting to consider that the constituent cells of such assemblies may change over time, given the known renewal and functional integration of newly generated granule cells (Cameron and McKay, 2001). This pattern of connectivity, with mossy fibers serving as intermediaries, could mediate the dye-coupling that has been observed between CA3 pyramidal cells (Dudek et al., 1983), though it would not explain reported dye-coupling between CA1 pyramidal cells or coupling between CA3 pyramidal cells in the dorsal hippocampus (Dudek et al., 1983; Baimbridge et al., 1991; Barnes et al., 1987). Precedence for mixed synapses serving as intermediaries for coupling between

neurons exists in the lateral vestibular nucleus of rat, where electrical coupling occurs between large vestibular neurons that themselves appear not to be connected by gap junctions; rather, the dendrites of different neurons locally form mixed synapses with branches of the same axon (Korn et al., 1973).

4. Experimental procedures

4.1. Animals and antibodies

All animals in this study were prepared under protocols approved by the Central Animal Care Services at the University of Manitoba. These protocols included minimization of stress to animals and minimization of number of animals used. A total of twelve adult male CD1 mice, two adult C57/BL6 wild-type and two Cx36 knockout mice, twenty adult male Sprague-Dawley rats, and four male Sprague-Dawley rats at postnatal day five were obtained from Central Animal Care Services at the University of Manitoba.

Primary antibodies used included two anti-Cx36 antibodies generated against different non-overlapping peptide sequences in Cx36 (monoclonal anti-Cx36 Ab39-4200 and polyclonal Ab51-6300), which were obtained from Life Technologies Corporation (formerly Invitrogen/Zymed, Carlsbad, CA, USA). The specificity of these antibodies has been previously established in various brain regions by showing presence vs. absence of immunofluorescence labelling for Cx36 in wild-type and Cx36 knockout mice, respectively (Li et al., 2004; Rash et al., 2004, 2007a,b). Additional primary antibodies employed were as follows: anti-vglut-1 obtained from Millipore (Temecula, CA, USA) and used at a dilution of 1:500; anti-AF6 and anti-ZO-1 obtained from Life Technologies Corp. and used at a concentration of 1 μg/ml and 3 μg/ml, respectively; anti-NR1 NMDA receptor subunit (NMDAR1) antibody obtained from Millipore (Temecula, CA, USA), used at a dilution of 1 μg/ml; and rabbit anti-parvalbumin generously provided by K. Baimbridge (University of British Columbia, Vancouver, Canada) and used at a dilution of 1:500. Secondary antibodies used included Cy3-conjugated goat or donkey anti-mouse IgG diluted 1:500 (Jackson ImmunoResearch Laboratories, West Grove, PA, USA), Alexa Flour 488-conjugated goat anti-rabbit and anti-mouse IgG diluted 1:1000 (Molecular Probes, Eugene, OR, USA), FITC-conjugated horse anti-mouse IgG diluted 1:100 (Vector Laboratories, Inc., Burlingame, CA, USA), Cy3-conjugated donkey anti-rabbit IgG diluted 1:200 (Jackson ImmunoResearch Laboratories) and Cy5-conjugated goat anti-guinea pig IgG diluted 1:200 (Jackson ImmunoResearch Laboratories). All antibodies were diluted in 50 mM Tris-HCl, pH 7.4, containing 1.5% sodium chloride (TBS) and 0.3% Triton X-100 (TBSTr) containing 10% normal goat or normal donkey serum.

4.2. Immunofluorescence labeling in hippocampus

Rats (200-300 g) and mice (30-35 g) were deeply anesthetized with equithesin (3 ml/kg) and transcardially perfused with 40 ml (for rats) or 3 ml (for mice) of prefixative solution consisting of cold (4°C) 25 mM sodium phosphate buffer (PB), pH 7.0, 0.9% NaCl, 0.1% sodium nitrite and heparin (1 unit/ml). This was followed by perfusion of rats with 200 ml and mice with 30 ml of cold 0.16 M sodium phosphate buffer, pH 7.0, containing either 1% or 2% formaldehyde (obtained from freshly depolymerized paraformaldehyde) and 0.2% picric acid. A final perfusion to wash out fixative consisted of cold PB containing 10% sucrose. Brains were removed and stored at 4°C for 48 h in cryoprotectant consisting of the final perfusate.

Sections of brain cut at a thickness of 10 to 15 μm were obtained using a cryostat, collected on gelatinized glass slides, and stored at -40 °C for use at a later date. Sections on slides were thawed, washed for 20 min in 50 mM Tris-HCl, pH 7.4, containing 1.5% sodium

chloride (TBS) and 0.3% Triton X-100 (TBSTr), and processed for immunofluorescence labelling as previously described (Li et al., 2008). For single labelling, sections were incubated for 24 h at 4°C with primary antibody, then washed for 1 h in TBSTr, and incubated for 1.5 h at room temperature with an appropriate secondary antibody. For double and triple immunofluorescence labelling, sections were incubated simultaneously with two or three primary antibodies for 24 h at 4°C, then washed for 1 h in TBSTr, and incubated for 1.5 h at room temperature simultaneously with appropriate combinations of secondary antibodies. After secondary antibody incubations, sections were washed in TBSTr for 20 min, then in 50 mM Tris-HCl buffer, pH 7.4, for 30 min, and covered with antifade medium and coverslipped. For double and triple immunofluorescence labelling, control procedures included omission of one of the primary antibodies with inclusion of each of the secondary antibodies to establish absence of inappropriate cross-reactions between primary and secondary antibodies or between different combinations of secondary antibodies.

An additional procedure was used for more detailed analyses of Cx36 localization in the dorsal-ventral (septo-temporal) and proximal-distal axes of the hippocampus. Four rats were euthanized, the hippocampus was removed and straightened to the extent possible along its septo-temporal axis, and immersion fixed in 2% formaldehyde containing 0.2% picric acid for 20 min. Following cryoprotection, the length of the hippocampus was measured and then sectioned in its entirety perpendicular to the septo-temporal axis. This allowed precise determination of the presence and distribution of Cx36-puncta in the stratum lucidum not only along the septo-temporal axis, but also in the stratum lucidum of hippocampal subfields CA3a, CA3b and CA3c in the proximal-distal (a.k.a. medial-lateral) dimension.

Fluorescence was examined on a Zeiss Axioskop2 fluorescence microscope with image capture using Axiovision 3.0 software (Carl Zeiss Canada, Toronto, Canada), and an Olympus Fluoview IX70 confocal microscope with image capture using Olympus Fluoview software. Images of immunolabelling obtained with Cy5 fluorochrome were pseudo colored blue. For confocal analysis, double-labelled sections were scanned twice using single laser excitation for each fluorochrome per scan, and data were collected either as single scan images or z-stack image of six to nine scans at z scanning intervals of typically 0.4 to 0.6 μm. Some z-stack images were reconstructed with rotation along the y-axis using Olympus Fluoview software. Images were assembled according to appropriate size and adjusted for contrast based on elimination of “empty” pixels using Adobe Photoshop CS (Adobe Systems, San Jose, CA, USA), and assembled using CorelDRAW Graphics Suite 12 (Corel Corporation, Ottawa, ON, Canada) and Northern Eclipse software (Empix Imaging, Mississauga, ON, Canada).

4.3. Quantitative analyses

For quantitative analysis and comparison of the densities of Cx36-immunopositive puncta in the hippocampal stratum lucidum (SL) and in the neuropil of the inferior olivary nucleus, tissues from four rats were prepared as above, immunolabelled for Cx36 and bassoon in the hippocampus and for Cx36 in the inferior olive, and examined by confocal laser scanning microscopy. Counts of Cx36-positive puncta were obtained in five to eight randomly selected volumes of the SL and inferior olive in each of the four rats. The puncta in areas of 80 × 80 μm in the x and y axis and 3.6 μm in the z axis were photographed and the images obtained were taken for counts. An estimate of the area of the SL containing immunofluorescence labelling for Cx36 was obtained using the immersion-fixed extended configuration of the hippocampus, with sections double-labelled for Cx36 and bassoon.

For quantitative estimates of the extent to which Cx36-puncta were co-localized with the mossy fiber terminal marker vglut-1 in the SL, a total of 54 randomly selected fields within the SL of two rats were photographed by confocal microscopy using single scans, and taken

for examination. Since many Cx36-positive puncta in the SL were very small, these tended to be obscured by usually intense labelling for vglut-1 in overlay images at sites where co-localization occurred, precluding counts of yellow puncta that result from spatial overlap of green and red pixels in digital overlays. Thus, quantitative data were acquired by transferring the locations of Cx36-puncta onto transparencies and overlaying these transparencies onto images of the same field displaying label for vglut-1. As a test for Cx36 co-localization with markers of mossy fiber terminals vs. simply coincidental overlap, images of mossy terminal markers from the same field double-labelled for Cx36 were flipped horizontally followed by comparison of co-localization in overlay images, as previously described (Li et al., 2008). Values for density of Cx36-puncta in the SL and the inferior olive, and those for the percentage co-localization of Cx36-puncta and vglut-1-positive mossy terminals, were determined for each field and expressed as mean ± s.e.m.

Supplementary Material

Refer to Web version on PubMed Central for supplementary material.

Acknowledgments

I thank B. McLean for excellent technical assistance and B.D. Lynn for help with the quantitative analyses. This work was supported by grants from the Canadian Institutes of Health Research to JIN, and from the National Institutes of Health (NS31027, NS44010, NS44395) to J.E. Rash with subaward to JIN.

Abbreviations

CNS	central nervous system
Cx36	connexin36
FRIL	freeze-fracture replica immunogold labelling
PV	parvalbumin
PCL	pyramidal cell layer
PB	25 mM sodium phosphate buffer
SL	stratum lucidum
TBSTr	50 mM Tris-HCl, pH 7.4, containing 1.5% sodium chloride (TBS) and 0.3% Triton X-100
TBS	50 mM Tris-HCl, pH 7.4, containing 1.5% sodium chloride
TEM	transmission electron microscopy
vglut-1	vesicular glutamate transporter-1
ZO-1	zonula occludens-1

REFERENCES

Acsady L, Kamondi A, Sik A, Freund T, Buzsaki G. GABAergic cells are the major postsynaptic targets of mossy fibers in the rat hippocampus. J. Neurosci. 1998; 18:3386–3403. [PubMed: 9547246]

Amaral DG, Dent JA. Development of the mossy fibers of the dentate gyrus1. A light and electron microscopic study of the mossy fibers and their expansions. J. Comp. Neurol. 1981; 195:51–86. [PubMed: 7204652]

Andrew RD, Taylor CP, Snow RW, Dudek FE. Coupling in rat hippocampal slices: dye transfer between CA1 pyramidal cells. Brain Res. Bull. 1982; 8:211–222. [PubMed: 6175384]

Baimbridge KG, Peet MJ, McLennan H, Church J. Bursting response to current-evoked depolariazation in rat CA1 pyramidal neurons is correlated with lucifer yellow dye coupling but not with the presence of calbindin-D28K. Synapse. 1991; 7:269–277. [PubMed: 2042109]

Barnes CA, Rao G, McNaughton BL. Increased electrotonic coupling in aged rat hippocampus: A possible mechanism for cellular excitability changes. J. Comp. Neurol. 1987; 259:549–558. [PubMed: 2439551]

Baude A, Bleasdale C, Dalezios Y, Somogyi P, Klausberger T. Immunoreactivity for GABAa receptor alpha1 subunit, somatostatin and connexin36 distinguishes axoaxonic, basket and bistratified interneurons of the rat hippocampus. Cereb. Cortex. 2007; 17:2094–2107. [PubMed: 17122364]

Belluardo N, Mud G, Trovato-Salinaro A, Gurun SL, Charollais A, Serre-Beinier V, Amato G, Haefliger JA, Meda P, Condorelli DF. Expression of connexin36 in the adult and developing rat brain. Brain Res. 2000; 865:121–138. [PubMed: 10814742]

Bennett MVL. Seeing is relieving: electrical synapses between visualized neurons. Nature Neurosci. 2000; 3:7–9. [PubMed: 10607387]

Bennett MVL, Zukin SR. Electrical coupling and neuronal synchronization in the mammalian brain. Neuron. 2004; 41:495–511. [PubMed: 14980200]

Bennett MVL, Pereda A. Pyramid power: Principal cells of thee hippocampus unite! Brain Cell Biol. 2006; 35:5–11. [PubMed: 17940909]

Bragdon AC, Taylor DM, Wilson WA. Potassium-induced epileptiform activity in area CA3 varies markedly along the septotemporal axis of the rat hippocampus. Brain Res. 1986; 378:169–173. [PubMed: 3742197]

Buhl DL, Harris KD, Hormuzdi SG, Monyer H, Buzsaki G. Selective impairment of hippocampal gamma oscillations in connexin36 knockout mouse in vivo. J. Neurosci. 2003; 23:1013–1018. [PubMed: 12574431]

Buzsaki G. Theta oscillations in the hippocampus. Neuron. 2002; 33:325–340. [PubMed: 11832222]

Cameron HA, McKay RD. Adult neurogenesis produces a large pool of new granule cells in the dentate gyrus. J. Comp. Neurol. 2001; 435:406–417. [PubMed: 11406822]

Chicurel ME, Harris KM. Three-dimensional analysis of the structure and composition of CA3 branched dendritic spines and their synaptic relationships with mossy fiber boutons in the rat hippocampus. J. Comp. Neurol. 1992; 325:169–182. [PubMed: 1460112]

Church J, Baimbridge KG. Exposure to high-pH medium increases the incidence and extent of dye coupling between rat hippocampus CA1 pyramidal neurons in vitro. J. Neurosci. 1991; 11:3289–32-95. [PubMed: 1941085]

Claiborne BJ, Amaral DG, Cowan WM. A light and electron microscopic analysis of the mossy fibers of the rat dentate gyrus. J. Comp. Neurol. 1986; 246:435–458. [PubMed: 3700723]

Condorelli DF, Parenti R, Spinella F, Salinaro AT, Belluardo N, Cardile V, Cicirata F. Cloning of a new gap junction gene (Cx36) highly expressed in mammalian brain neurons. Eur. J. Neurosci. 1998; 10:1202–1208. [PubMed: 9753189]

Condorelli DF, Belluardo N, Trovato-Salinaro A, Mudo G. Expression of Cx36 in mammalian neurons. Brain Res. Rev. 2000; 32:72–85. [PubMed: 10751658]

Connors BW, Long MA. Electrical synapses in the mammalian brain. Annu. Rev. Neurosci. 2004; 27:393–418. [PubMed: 15217338]

Csicsvari J, Hirase H, Mamiya A, Buzsaki G. Ensemble patterns of hippocampal CA3–CA1 neurons during sharp wave-associated population events. Neuron. 2000; 28:585–594. [PubMed: 11144366]

Csicsvari J, Jamieson B, Wise KD, Buzsaki G. Mechanisms of gamma oscillations in the hippocampus of the behaving rat. Neuron. 2003; 37:311–322. [PubMed: 12546825]

Degen J, Meier C, van der Giessen RS, Sohl G, Petrasch-Parwez E, Urschel S, Dermietzel R, Schilling K, de Zeeuw CI, Willecke K. Expression pattern of lacZ reporter gene representing connexin36 in transgenic mice. J. Comp. Neurol. 2004; 473:511–525. [PubMed: 15116387]

Derchansky M, Rokni D, Rick JT, Wennberg R, Bardakjian BL, Zhang L, Yarom Y, Carlen PL. Bidirectional Multisite Seizure Propagation in the Intact Isolated Hippocampus: The multifocality of the seizure focus. Neurobiol. Disease. 2006; 23:312–28.

Dudek, FE.; Andrew, RD.; MacVicar, BA.; Snow, RW.; Taylor, CP. Recent evidence for and possible significance of gap junctions and electrotonic synapses in the mammalian brain.. In: Jasper, HH.;

van Gelder, NM., editors. Basic Mechanisms of Neuronal Hyperexcitability. Liss; New York: 1983. p. 31-73.

Fukuda T, Kosaka T. Gap junctions linking the dendritic network of GABAergic interneurons in the hippocampus. J. Neurosci. 2000; 20:1519–1528. [PubMed: 10662841]

Fulton BP. Gap junctions in the developing nervous system. Perspect. Dev. Neurobiol. 1995; 2:327–334. [PubMed: 7538866]

Gilbert M, Racine RJ, Smith GK. Epileptiform burst responses in ventral vs dorsal hippocampal slices. Brain Res. 1985; 361:389–391. [PubMed: 4084805]

Hagiwara A, Fukazawa Y, Deguchi-Tawarada M, Ohtsuka T, Shigemoto R. Differential Distribution of Release-Related Proteins in the Hippocampal CA3 Area as Revealed by Freeze-Fracture Replica Labeling. J. Comp. Neurol. 2005; 489:195–216. [PubMed: 15983999]

Hamzei-Sichani F, Kamasawa N, Janssen WGM, Yasumura T, Davidson KGV, Hof PR, Wearne SL, Stewart MG, Young SR, Whittington MA, Rash JE. Gap junctions on hippocampal mossy fiber axons demonstrated by thin-section electron microscopy and freeze-fracture replica immunogold labeling. Proc. Natl. Acad. Sci. (USA). 2007; 104:12548–12553. [PubMed: 17640909]

Hempelmann A, Heils A, Sander T. Confirmatory evidence for an association of the connexin36 gene with juvenile myoclonic epilepsy. Epilepsy Res. 2006; 71:223–228. [PubMed: 16876983]

Hormuzdi SG, Pais I, LeBeau FE, Towers SK, Rozov A, Buhl EH, Whittington MA, Monyer H. Impaired electrical signaling disrupts gamma frequency oscillations in connexin 36-deficient mice. Neuron. 2001; 31:487–495. [PubMed: 11516404]

Hormuzdi SG, Filippov MA, Mitropoulon G, Monyer H, Bruzzone R. Electrical synapses: a dynamic signaling system that shapes the activity of neuronal networks. Biochem. Biophys. Acta. 2004; 1662:113–137. [PubMed: 15033583]

Inagari M, Irie K, Deguchi-Tawarada M, Ikeda W, Ohtsuka T, Takeuchi M, Takai W. Nectin-dependent localization of ZO-1 at puncta adhaerentia junctions between the mossy fiber terminals and the dendrites of the pyramidal cells in the CA3 area of adult mouse hippocampus. J. Comp. Neurol. 2003; 460:514–524. [PubMed: 12717711]

Ishizuka N, Cowan WM, Amaral DB. A quantitative analysis of the dendritic organization of pyramidal cells in the rat hippocampus. J. Comp. Neurol. 1995; 362:17–45. [PubMed: 8576427]

Jaffe DB, Gutierrez R. Mossy fiber synaptic transmission: communication from the dentate gyrus. Prog. Brain Res. 2007; 163:109–132. [PubMed: 17765714]

Kamasawa N, Furman CS, Davidson KGV, Sampson JA, Magnie AR, Gebhardt BR, Kamasawa M, Yasumura T, Zumbrunnen JR, Pickard GE, Nagy JI, Rash JE. Abundance and ultrastructural diversity of neuronal gap junctions in the OFF and ON sublaminae of the inner plexiform layer of rat and mouse retina. Neuroscience. 2006; 142:1093–1117. [PubMed: 17010526]

Kaneko T, Fujiyama F, Hioki H. Immunohistochemical localization of candidates for vesicular glutamate transporters in the rat brain. J. Comp. Neurol. 2002; 444:39–62. [PubMed: 11835181]

Katsumaru H, Kosaka T, Heizmann CW, Hama K. Gap junctions on GABAergic neurons containing the calcium-binding protein parvalbumin in the rat hippocampus (CA1 region). Exp. Brain Res. 1988; 72:363–370. [PubMed: 3066635]

Korn H, Sotelo C, Crepel F. Electrotonic coupling between neurons in the lateral vestibular nucleus. Exp. Brain Res. 1973; 16:255–275. [PubMed: 4346867]

Kosaka T. Gap junctions between non-pyramidal cell dendrites in the rat hippocampus (CA1 and CA3 regions). Brain Res. 1983a; 271:157–161. [PubMed: 6883113]

Kosaka T. Neuronal gap junctions in the polymorph layer of the rat dentate gyrus. Brain Res. 1983b; 277:347–351. [PubMed: 6640301]

Kosaka T, Hama K. Gap junctions between non-pyramidal cell dendrites in the rat hippocampus (CA1 and CA3 regions): a combined golgi-electron microscopy study. J. Comp. Neurol. 1985; 231:150–161. [PubMed: 3968232]

Lee PH, Xie CW, Lewis DV, Wilson WA, Mitchell CL, Hong JS. Opioid-induced epileptiform bursting in hippocampal slices: higher susceptibility in ventral than dorsal hippocampus. J. Pharmacol. Exp. Ther. 1990; 253:545–551. [PubMed: 2159997]

Li X, Olson C, Lu S, Kamasawa N, Yasumura T, Rash JE, Nagy JI. Neuronal connexin36 association with zonula occludens-1 protein (ZO-1) in mouse brain and interaction with the first PDZ domain of ZO-1. Eur. J. Neurosci. 2004; 19:2132–2146. [PubMed: 15090040]

Li X, Kamasawa N, Ciolofan C, Olson CO, Lu S, Davidson KGV, Yasumura T, Shigemoto R, Rash JE, Nagy JI. Connexin45-containing neuronal gap junctions in rodent retina also contain connexin36 in both apposing hemiplaques, forming bi-homotypic gap junctions, with scaffolding contributed by zonula occludens-1. J. Neurosci. 2008; 28:9769–89. [PubMed: 18815262]

Li X, Lynn BD, Nagy JI. The effector protein AF6 and scaffolding multi-PDZ domain protein 1 (MUPP1) interact with connexin36 and are localized at electrical synapses in adult rodent. Eur. J. Neurosci. 2011 In Press.

MacVicar BA, Dudek FE. Electrotonic coupling between pyramidal cells: a direct demonstration in rat hippocampal slices. Science. 1981; 213:782–785. [PubMed: 6266013]

Maier N, Guldenagel M, Sohl G, Siegmund H, Willecke K, Graguhn A. Reduction of high-frequency network oscillations (ripples) and pathological network discharges in hippocampal slices from connexin36- deficient mice. J. Physiol. 2002; 541:521–528. [PubMed: 12042356]

Mas C, Taske N, Seutsch S, Guipponi M, Thomas P, Covanis A, Friis M, Kjeldsen MJ, Pizzonlato GP, Villenure JG, Buresi C, Rees M, Malafosse A, Gardiner M, Antonarakis SE, Meda P. Association of the connexin36 gene with juvenile myoclonic epilepsy. J. Med. Genet. 2004; 41:93.

Mercer A, Bannister AP, Thomson AM. Electrical coupling between pyramidal cells in adult cortical regions. Brain Cell. Biol. 2006; 35:13–27. [PubMed: 17940910]

Meyer AH, Katona I, Blatow M, Rozov A, Monyer H. In vitro labeling of parvalbumin-positive interneurons and analysis of electrical coupling in identified neurons. J. Neurosci. 2002; 22:7055–7064. [PubMed: 12177202]

Montoro RJ, Yuste R. Gap junctions in developing neocortex: a review. Brain Res. Rev. 2004; 47:216–226. [PubMed: 15572173]

Nagy, JI.; Dermietzel, R. Gap junctions and connexins in the mammalian central nervous system.. In: Hertzberg, EL., editor. Advances in Molecular and Cell Biology. Vol. 30. JAI Press Inc; NY: 2000. p. 323-396.

Nishioka H, Mizoguchi A, Nakanishi H, Mandai K, Takahashi K, Kimura K, Satoh-Moriya A, Takai Y. Localization of l-afadin at puncta adhaerentia-like junctions between the mossy fiber terminals and the dendritic trunks of pyramidal cells in the adult mouse hippocampus. J. Comp. Neurol. 2000; 424:297–306. [PubMed: 10906704]

Papatheodoropoulos C, Kostopoulos G. Dorsal-ventral differentiation of short-term synaptic plasticity in rat CA1 hippocampal region. Neurosci. Lett. 2000; 286:57–60. [PubMed: 10822152]

Papatheodoropoulos C, Kostopoulos G. Spontaneous GABA(A)-dependent synchronous periodic activity in adult rat ventral hippocampal slices. Neurosci. Lett. 2002a; 319:17–20. [PubMed: 11814643]

Papatheodoropoulos C, Kostopoulos G. Spontaneous, low frequency (approximately 2 – 3 Hz) field activity generated in rat ventral hippocampal slices perfused with normal medium. Brain Res. Bull. 2002b; 57:187–193. [PubMed: 11849825]

Papatheodoropoulos C, Asprodini E, Nikita I, Koutsona C, Kostopoulos G. Weaker synaptic inhibition in CA1 region of ventral compared to dorsal rat hippocampal slices. Brain Res. 2002; 948:117–121. [PubMed: 12383962]

Papatheodoropoulos C, Moschovos C, Kostopoulos G. Greater contribution of N-methyl-d-aspartic acid receptors in ventral compared to dorsal hippocampal slices in the expression and long-term maintenance of epileptiform activity. Neuroscience. 2005; 135:765–779. [PubMed: 16154282]

Paxinos, G.; Watson, JD. The rat brain in stereotaxic coordinates. Academic Press; NY: 1986.

Pereda A, O'Brian JO, Nagy JI, Bukauskas F, Davidson KGV, Yasumura T, Rash JE. Connexin35 mediates electrical transmission at mixed synapses on Mauthner cells. J. Neurosci. 2003; 23:7489–7503. [PubMed: 12930787]

Pereda A, Rash JE, Nagy JI, Bennett MVL. Dynamics of electrical transmission at club endings on the Mauthner cells. Brain Res. Rev. 2004; 47:227–244. [PubMed: 15572174]

Perez Velazquez JL, Carlen PL. Gap junctions, synchrony and seizures. Trends Neurosci. 2000; 23:68–74. [PubMed: 10652547]

Pike FG, Goddard RS, Suckling JM, Ganter P, Kasthuri N, Paulsen O. Distinct frequency preferences of different types of rat hippocampal neurones in response to oscillatory input currents. J. Physiol. 2000; 529:205–213. [PubMed: 11080262]

Racine R, Rose PA, Burnham WM. Afterdischarge thresholds and kindling rates in dorsal and ventral hippocampus and dentate gyrus. Can. J. Neurol. Sci. 1977; 4:273–278. [PubMed: 597802]

Rash JE, Dillman RK, Bilhartz BL, Duffy HS, Whalen LR, Yasumura T. Mixed synapses discovered and mapped throughout mammalian spinal cord. Proc. Nat. Acad. Sci. (USA). 1996; 93:4235–4239. [PubMed: 8633047]

Rash JE, Yasumura T, Dudek FE. Ultrastructure, histological distribution, and freeze-fracture immunocytochemistry of gap junctions in rat brain and spinal cord. Cell Biol. Int. 1998; 22:731–749. [PubMed: 10873288]

Rash JE, Staines WA, Yasumura T, Pate D, Hudson CS, Stelmack GL, Nagy JI. Immunogold evidence that neuronal gap junctions in adult rat brain and spinal cord contain connexin36 (Cx36) but not Cx32 or Cx43. Proc. Natl. Acad. Sci. (USA). 2000; 97:7573–7578. [PubMed: 10861019]

Rash JE, Yasumura T, Dudek FE, Nagy JI. Cell-specific expression of connexins, and evidence for restricted gap junctional coupling between glial cells and between neurons. J. Neurosci. 2001; 21:1983–2000. [PubMed: 11245683]

Rash JE, Pereda A, Kamasawa N, Furman CS, Yasumura T, Davidson KGV, Dudek FE, Olson C, Li X, Nagy JI. High-resolution proteomic mapping in the vertebrate central nervous system: Close proximity of connexin35 to NMDA glutamate receptor clusters and co-localization of connexin36 with immunoreactivity for zonula occludens protein-1 (ZO-1). J. Neurocytol. 2004; 33:131–151. [PubMed: 15173637]

Rash JE, Olson CO, Pouliot WA, Davidson KGV, Yasumura T, Furman CS, Royer S, Kamasawa N, Nagy JI, Dudek FE. Connexin36, miniature neuronal gap junctions, and limited electrotonic coupling in rodent suprachiasmatic nucleus (SCN). Neuroscience. 2007a; 149:350–371. [PubMed: 17904757]

Rash JE, Olson CO, Davidson KGV, Yasumura T, Kamasawa N, Nagy JI. Identification of connexin36 in gap junctions between neurons in rodent locus coeruleus. Neuroscience. 2007b; 147:938–956. [PubMed: 17601673]

Ribak CE, Seress L, Leranth C. Electron microscopic distribution of parvalbumin-containing neurons and axon terminals in the primate dentate gyrus and ammon's horn. J. Comp. Neurol. 1993; 327:298–321. [PubMed: 8425946]

Richter K, Langnaese K, Kreutz MR, Olias G, Zhai R, Scheich H, Garner CC, Gundelfinger ED. Presynaptic cytomatrix protein bassoon is localized at both excitatory and inhibitory synapses of rat brain. J. Comp. Neurol. 1999; 408:437–448. [PubMed: 10340516]

Rollenhagen A, Lubke JHR. The mossy fiber bouton: the common or the unique synapse. Front. Synaptic Neurosci. 2010; 2:1–9. [PubMed: 21423487]

Rouach N, Avignone E, Meme W, Koulafoff A, Venance L, Blomstrand F, Giaume C. Gap junctions and connexin expression in the normal and pathological central nervous system. Biol. Cell. 2002; 94:457–475. [PubMed: 12566220]

Scharman HE. Spiny neurons of area CA3c in rat hippocampal slices have similar electrophysiological characteristics and synaptic responses despite morphological variation. Hippocampus. 1993; 3:9–28. [PubMed: 8364685]

Schmalbruch H, Jahnsen H. Gap junctions on CA3 pyramidal cells of guinea pig hippocampus by freeze-fracture. Brain Res. 1981; 217:175–178. [PubMed: 7260615]

Schmitz D, Schuchmann S, Fisahn A, Draguhn A, Buhl EH, Petrasch-Parwez E, Dermietzel R, Heinemann U, Traub RD. Axo-Axonal coupling: a novel mechanism of ultrafast neuronal communication. Neuron. 2001; 31:831–840. [PubMed: 11567620]

Siegel SJ, Brose N, Janssen WG, Gasic GP, Jahn R, Heinemann SF, Morrison JH. Regional, cellular, and ultrastructural distribution of N-methyl-D-aspartate receptor subunit 1 in monkey hippocampus. Proc. Natl. Acad. Sci. USA. 1994; 91:564–568. [PubMed: 8290563]

Sohl G, Degen J, Teubner B, Willecke K. The murine gap junction gene connexin36 is highly expressed in mouse retina and regulated during brain development. FEBS Lett. 1998; 428:27–31. [PubMed: 9645468]

Sohl G, Odermatt B, Maxeiner S, Degen J, Willecke K. New insights into the expression and function of neural connexins with transgenic mouse mutants. Brain Res. Rev. 2004; 47:245–259. [PubMed: 15572175]

Sotiriou E, Papatheodoropoulos C, Angelatou F. Differential expression of gamma-aminobutyric acid-A receptor subunits in rat dorsal and ventral hippocampus. J. Neurosci. Res. 2005; 82:690–700. [PubMed: 16273537]

tom Dieck S, Sanmarti-Vila L, Langnaese K, Richter K, Kindler S, Soyke A, Wex H, Smalla KH, Kampf U, Franzer JT, Stumm M, Garner CC, Gundelfinger ED. Bassoon, a novel zinc-finger CAG/glutamine-repeat protein selectively localized at the active zone of presynaptic nerve terminals. J. Cell Biol. 1998; 142:499–509. [PubMed: 9679147]

Traub RD, Whittington MA, Colling SB, Buzsaki G, Jefferys JG. Analysis of gamma rhythms in the rat hippocampus in vitro and in vivo. J. Physiol. 1996; 493:471–484. [PubMed: 8782110]

Traub RD, Whittington MA, Buhl EH, LeBeau FE, Bibbig A, Boyd S, Cross H, Baldeweg T. A possible role for gap junctions in generation of very fast EEG oscillations preceding the onset of, and perhaps initiating, seizures. Epilepsia. 2001; 42:153–170. [PubMed: 11240585]

Watanabe M, Fukaya M, Sakimura K, Manabe T, Mishina M, Inoue Y. Selective scarcity of NMDA receptor channel subunits in the stratum lucidum (mossy fibre-recipient layer) of the mouse hippocampal CA3 subfield. Eur. J. Neurosci. 1998; 10:478–487. [PubMed: 9749710]

Whishaw IQ, Metz GAS, Kolb B, Pellis SM. Accelerated nervous system development contributes to behavioral efficiency in the laboratory mouse: a behavioral review and theoretical proposal. Dev. Psychobiol. 2001; 39:151–170. [PubMed: 11745309]

Witter, MP.; Amaral, DG. Hippocampal formation.. In: Paxinos, G., editor. The rat nervous system. Elsevier Academic Press; Amsterdam: 2004. p. 635-704.

Zsiros V, Maccaferri G. Electrical coupling between interneurons with different excitable properties in the stratum lacunosum-moleculare of the juvenile CA1 rat hippocampus. J. Neurosci. 2005; 21:86–95.

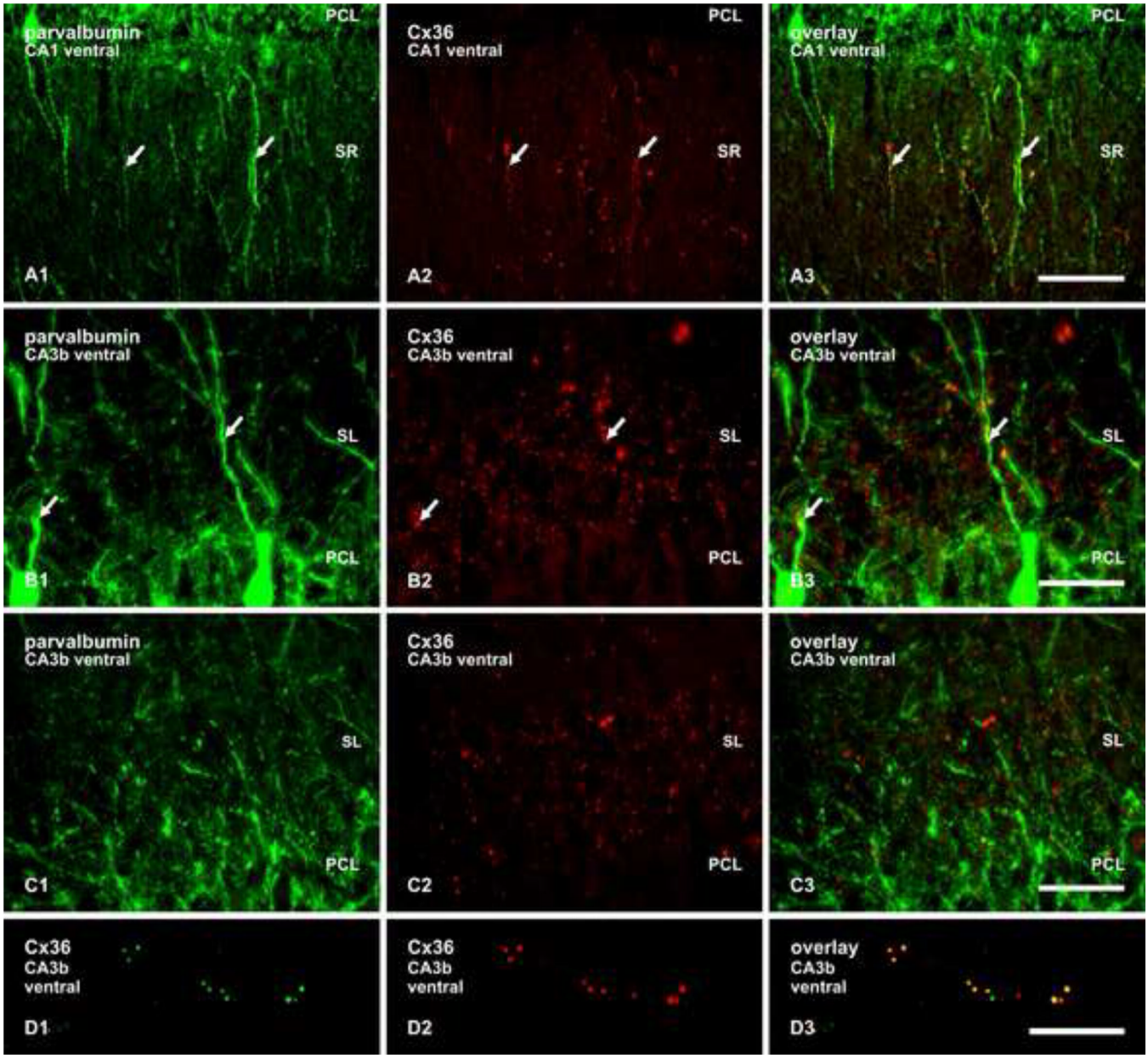

Fig. 1.

Double immunofluorescence labelling of Cx36 and PV in adult rat ventral hippocampus. (A) Images of the same field (A1-A3) in the ventral hippocampal CA1 area, showing PV-immunoreactive dendrites (A1, arrows) extending into the stratum radiatum (SR) from PV-positive neurons in the pyramidal cell layer (PCL), with linear arrays of Cx36-positive puncta (A2, arrows) localized along these dendrites, as seen in overlay (A3, arrows). (B) Images of the same field (B1-B3) in the ventral hippocampal CA3b area adjacent to the PCL, showing PV-positive dendrites (B1, arrows) extending into the stratum lucidum (SL) from their cell bodies in the PCL, and a small number of large Cx36-puncta (B1, arrows) (labeled with Ab39-4200) localized along these dendrites, as seen in overlay (B3, arrows). A much higher density of very fine Cx36-positive puncta in the SL show lack of overlap with PV-positive fibers. (C) Images of a similar field as in B, but immunolabelled for Cx36 with polyclonal anti-Cx36 Ab51-6300 generated against a different sequence in Cx36 than

monoclonal Ab39-4200, again showing PV-immunoreactive fibers (C1) largely lacking co-localization with fine Cx36-puncta (C2, and overlay in C3) in the SL. (D) Confocal double immunofluorescence of the same field in SL (D1-D3), showing that Cx36-puncta labelled with Ab39-4200 (D1) correspond to those labelled with Ab51-6300 (D2), as seen in overlay (D3). Scale bars: A, 100 m; B,C, 50 μm; D, 10 μm.

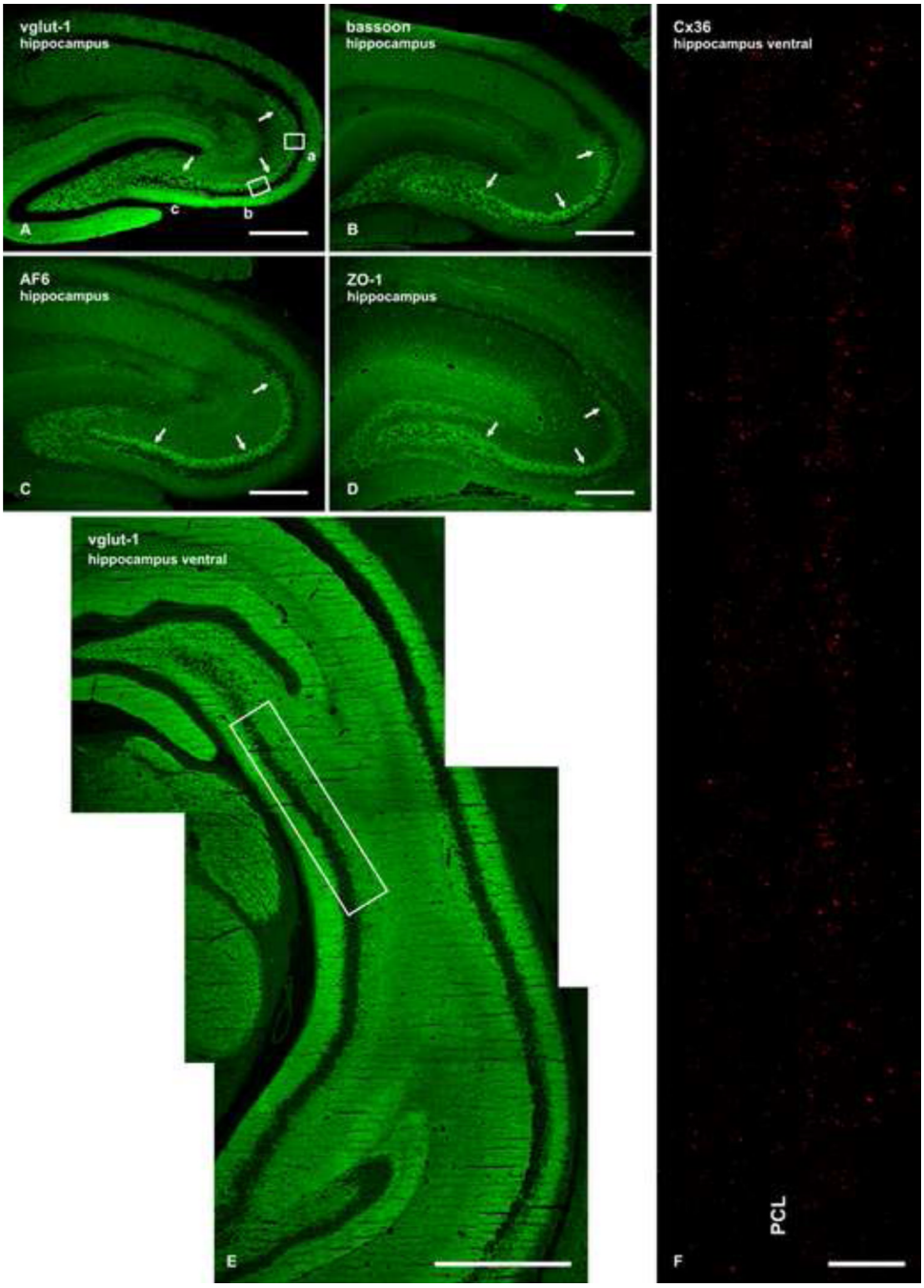

Fig. 2.

(A-D) Immunofluorescence for vglut-1 (A), bassoon (B), AF6 (C) and ZO-1 (D) in adult rat hippocampus, showing intense labelling for each of these proteins in the SL (arrows) of hippocampal subregions CA3a, CA3b and CA3c (indicated in A). (E) Low magnification of ventral hippocampus immunolabelled for vglut-1, with boxed area indicating location of image shown in F. (F) Single scan low magnification confocal photomontage showing immunolabelling of Cx36 associated with a 1.7 mm length along the SL in CA3b of rat ventral hippocampus. At this rostro-caudal level, the SL straddles each side of the PCL and is heavily invested with Cx36-positive puncta. Some puncta are also seen very sparsely distributed within the PCL. Scale bars: A-D, 500 μm; E, 1 mm; F, 100 μm.

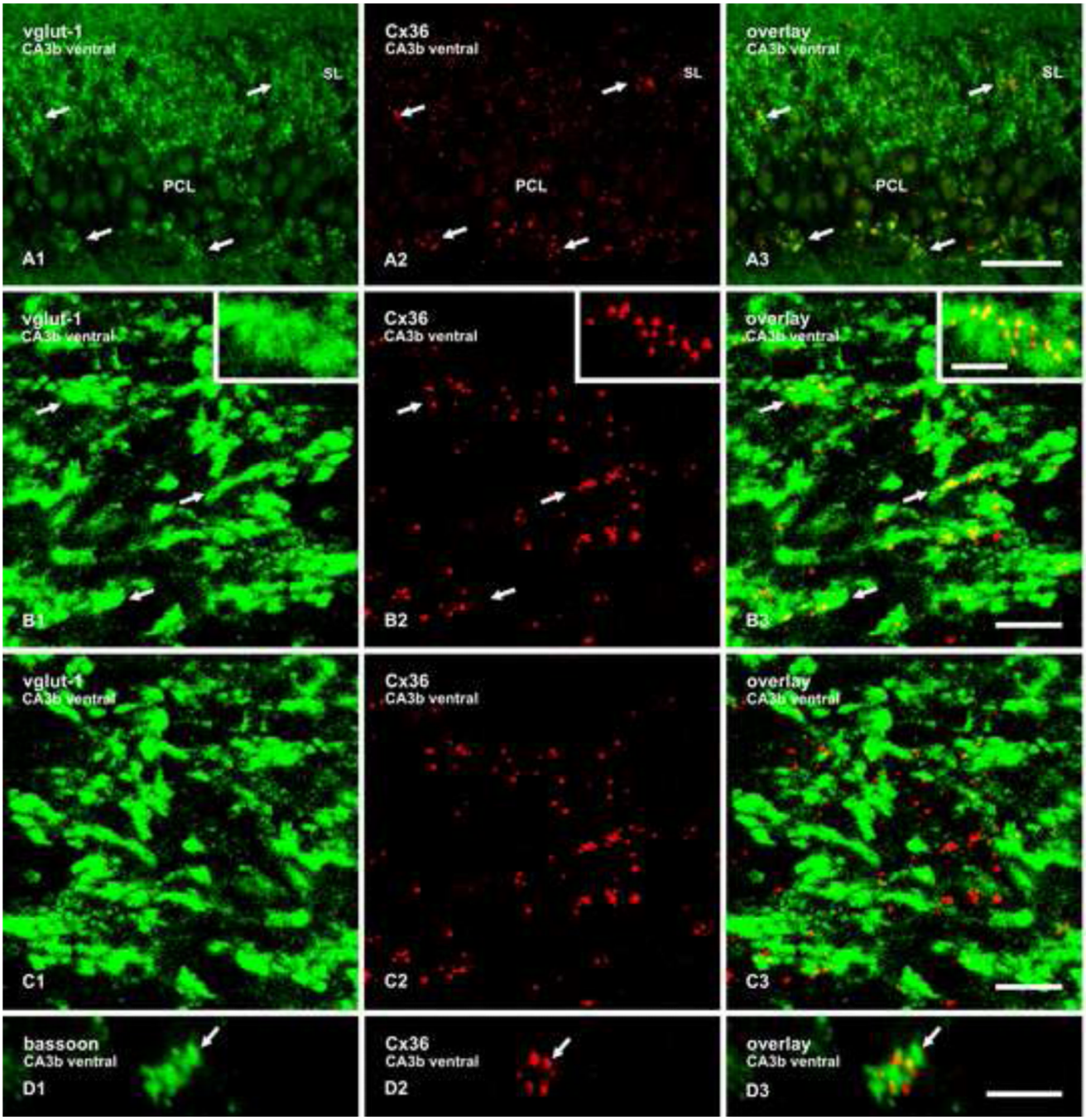

Fig. 3.

Double immunofluorescence labelling of Cx36 and vglut-1 in the SL of the CA3b region of adult rat ventral hippocampus. (A1-A3) Images of the same field, showing dense labelling for vglut-1 in mossy fiber terminals (A1, arrows), and Cx36-positive puncta straddling the CA3b region of the PCL (A2, arrows), where these puncta are co-distributed with immunolabelling for vglut-1, as seen in overlay (A3, arrows). (B1-B3) Confocal double immunofluorescence labelling in a z-stack of nine scans in an area of SL similar to that in (A), showing co-localization of vglut-1-positive terminals (B1, arrows; magnified in inset) with Cx36-positive puncta (B2, arrows), as seen in overlay (B3, arrows). (C) The same set of images as in B, showing minimal vglut-1/Cx36 co-localization (C3) after horizontal 180°

flip of the image displaying vglut-1 in B1. (D) Confocal double immunofluorescence, showing co-localization of the nerve terminal marker bassoon (D1, arrow) with Cx36 (D2, arrow), as seen in overlay (D3, arrow). Scale bars: A, 50 m; B,C 10 m; D and inset in B, 5 μm.

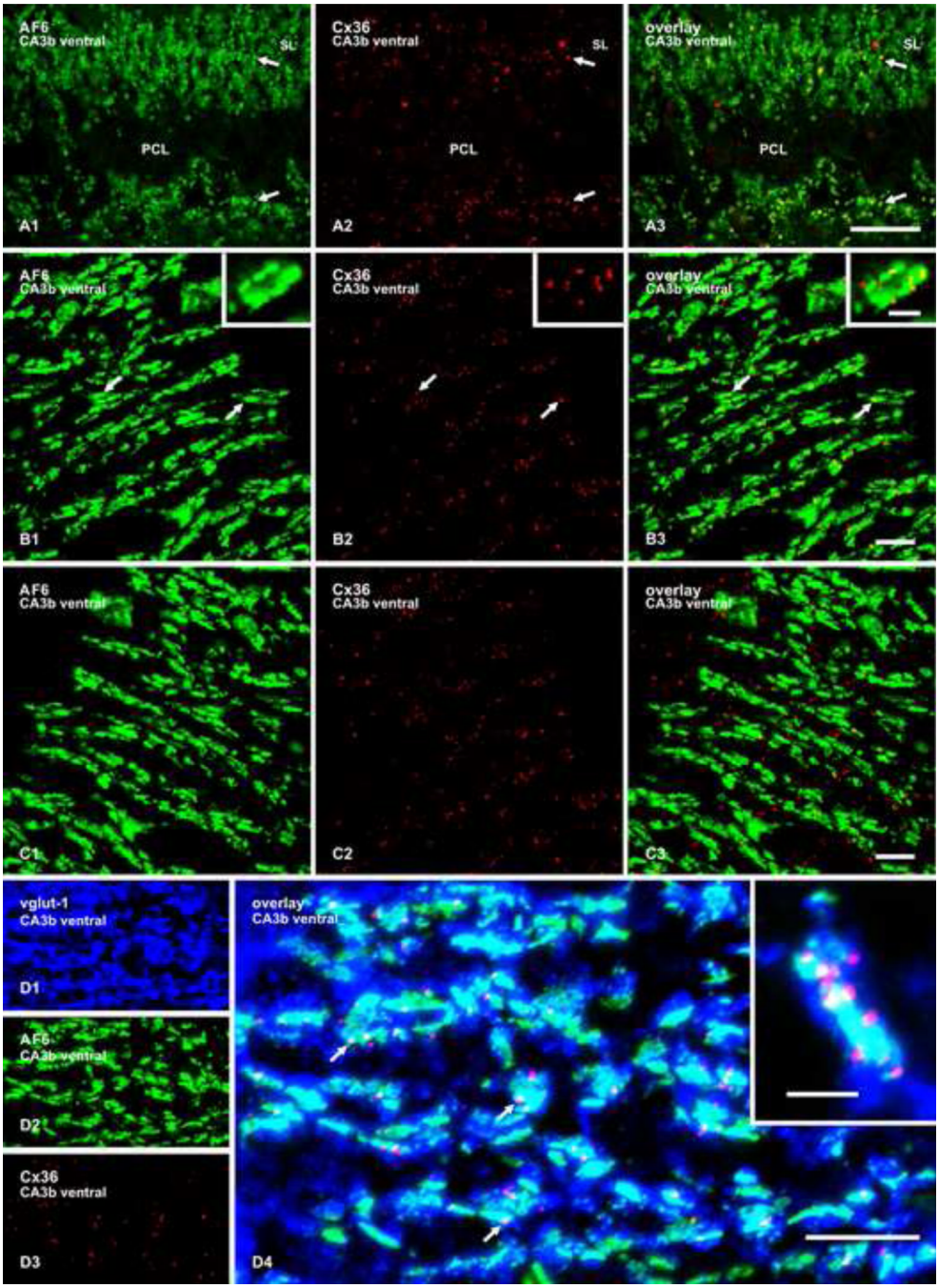

Fig. 4.

Double and triple immunofluorescence labelling of AF6, Cx36 and vglut-1 in the SL of the CA3b region in adult rat ventral hippocampus. (A1-A3) The same field, showing AF6 in mossy fiber terminals (A1, arrows), and Cx36-puncta on each side of the PCL (A2, arrows) co-distributed with labelling for AF6, as seen in overlay (A3, arrows). (B1-B3) Confocal double immunofluorescence in a z-stack of seven scans in an area of the SL similar to that in (A), showing co-localization of AF6 (B1, arrows; magnified in inset) with Cx36 (B2, arrows), as seen in overlay (B3, arrows). (C) The same set of images as in B, showing greatly reduced AF6/Cx36 co-localization (C3) after horizontal 180° flip of the image in B1. (D1-D4) Confocal triple immunofluorescence in a z-stack of eight scans showing the same

field labelled for vglut-1 (D1), AF6 (D2) and Cx36 (D3), with co-localization of the three labels shown in overlay (D4, arrows), and at higher magnification in inset. Cx36-puncta (red) are often seen at the edges of AF6-positive patches (green) that are associated with mossy terminals (blue). Scale bars: A, 50 μm; B,C,D, 10 μm; inset in B and D, 3 μm.

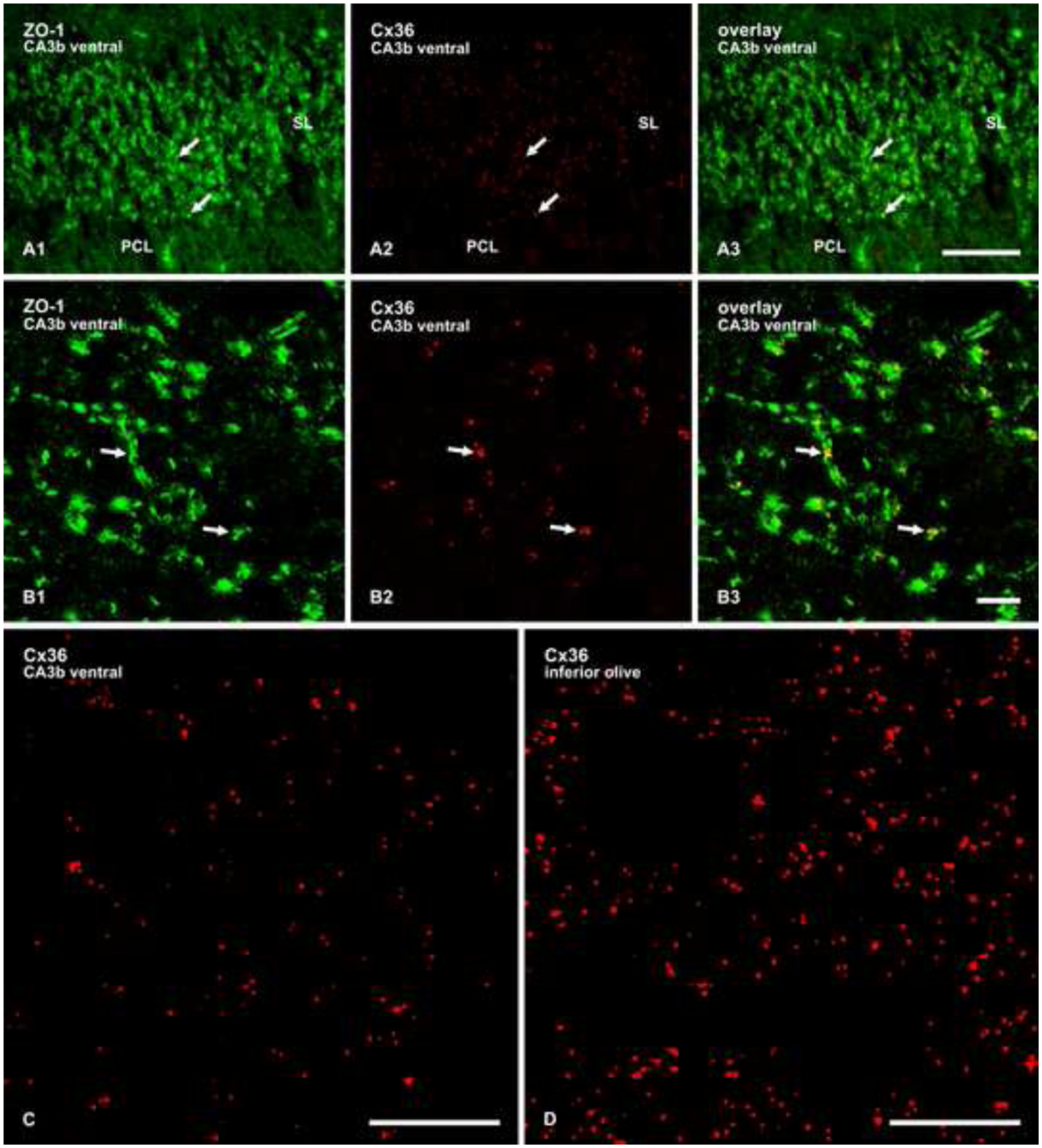

Fig. 5.

(A,B) Double immunofluorescence labelling of ZO-1 and Cx36 in the SL of the CA3b region of adult rat ventral hippocampus. (A1-A3) The same field, showing ZO-1 in mossy fiber terminals (A1, arrows) and Cx36-puncta (A2, arrows) co-distributed with labelling for ZO-1 in the SL, as seen in overlay (A3, arrows). (B1-B3) Confocal double immunofluorescence in a z-stack of six scans in an areas of SL similar to that in A, showing punctate labelling for ZO-1 (B1, arrows) co-localized with Cx36-positive puncta (B2, arrows), as seen in overlay (B3, arrows). C,D, Confocal immunofluorescence labelling for Cx36, showing examples of images used for quantitative analysis of the density of Cx36-

positve puncta in the SL (C) and the inferior olivary nucleus (D). Scale bars: A, 50 μm; B, 10 μm; C,D, 20 μm.

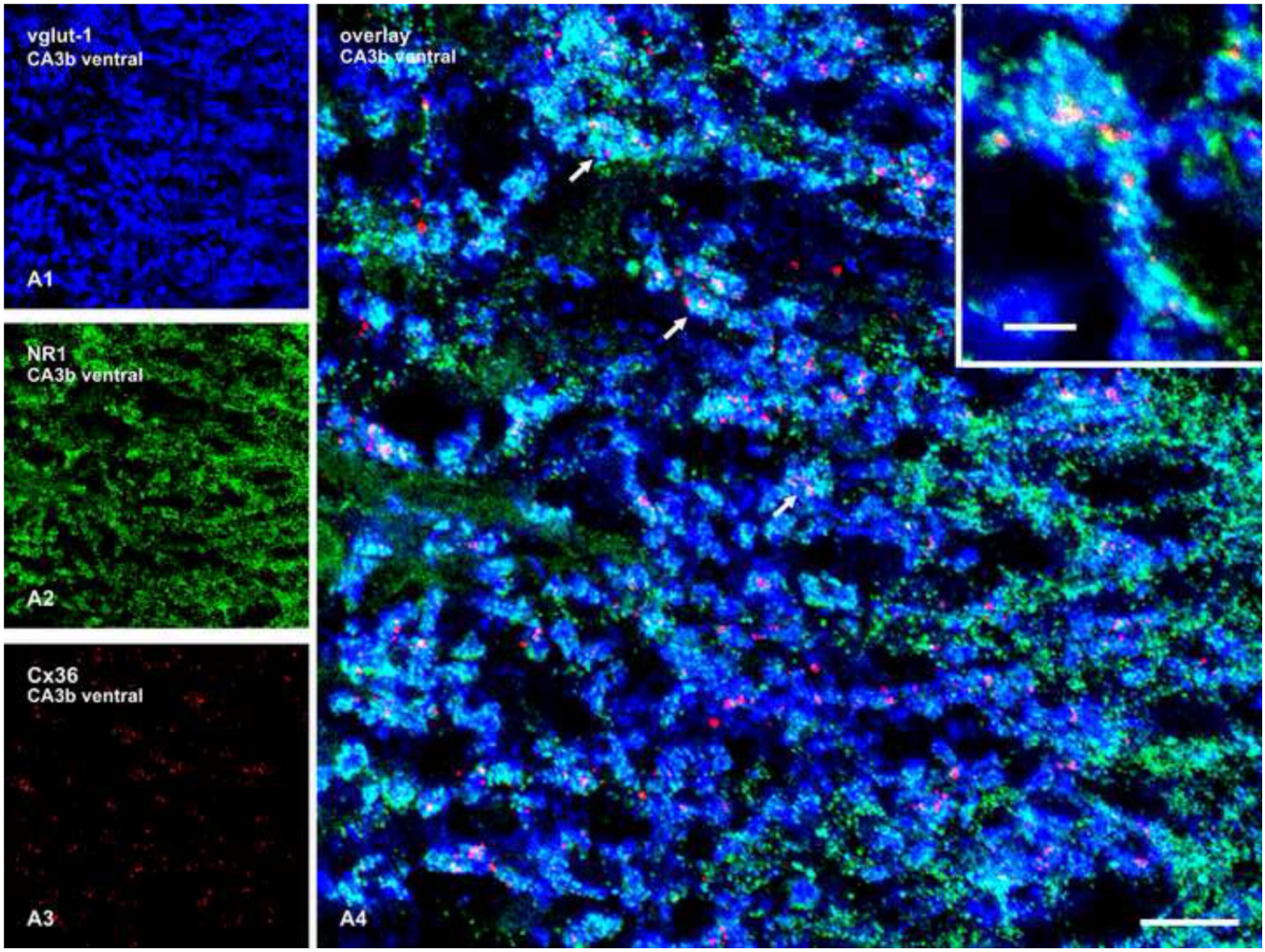

Fig. 6.

Confocal triple immunofluorescence in a z-stack of five scans showing the same field labelled for vglut-1 (A1), NR1 (A2) and Cx36 (A3), with co-distribution of the three labels shown in overlay (A4), and at higher magnification in inset. Cx36-positive puncta (red) associated with vglut-1-positive mossy terminals (blue) are often seen intermingled with clusters of NR1-positive puncta (green), as seen in overlay (A4, arrows, and inset). Scale bars: A4, 10 μm, and 3 μm in inset.

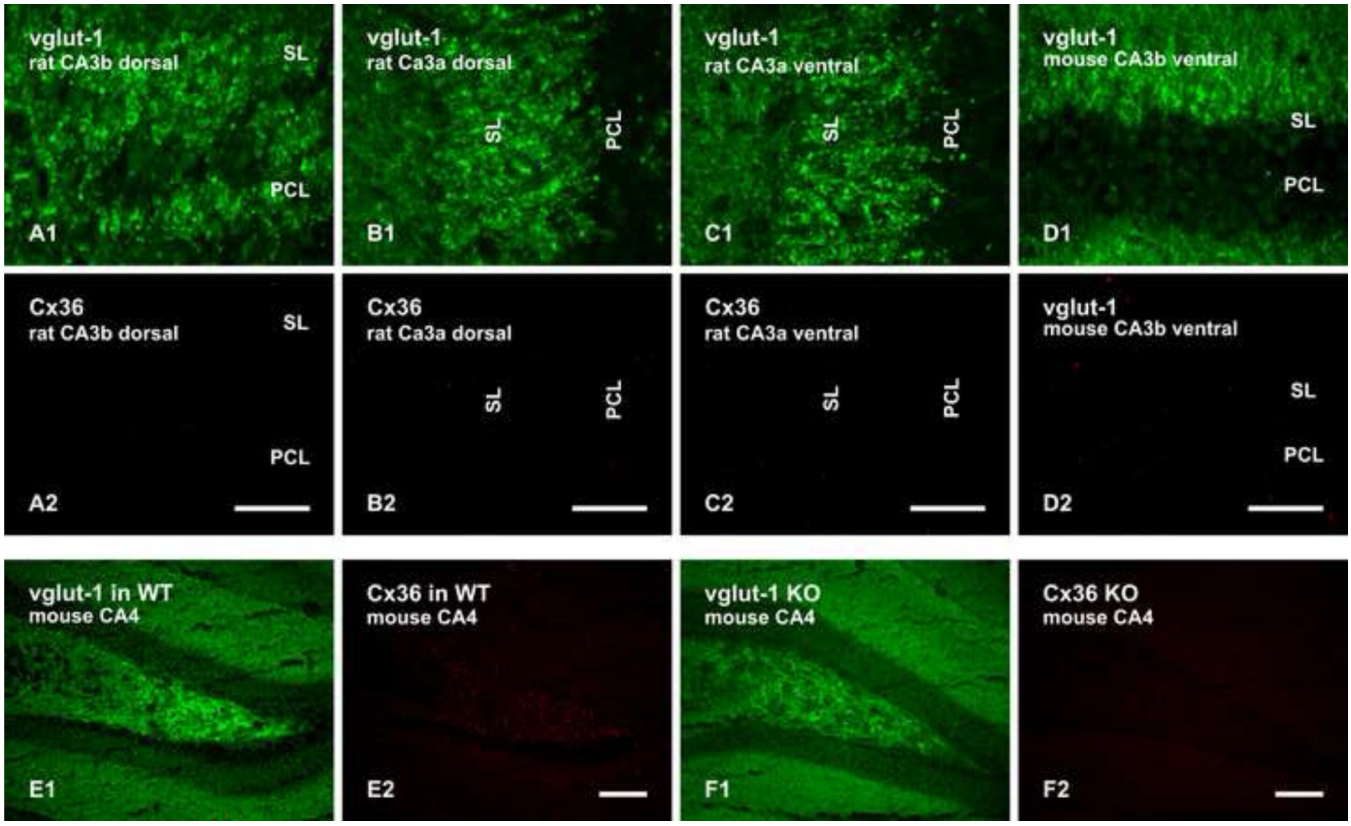

Fig. 7.

Section processed for double immunofluorescence labelling of vglut-1 and Cx36 in various hippocampal subregions of adult rat and mouse. (A1,A2) The same field, with labelling for vglut-1 and Cx36 in SL of CA3b in rat dorsal hippocampus. (B1,B2) The same field, with labelling for vglut-1 and Cx36 in SL of CA3a in rat dorsal hippocampus. (C1,C2) The same field, with labelling for vglut-1 and Cx36 in SL of CA3a in rat ventral hippocampus. (D1,D2) The same field, with labelling for vglut-1 and Cx36 in SL of CA3b in mouse ventral hippocampus. The SL in each of the regions shown in A-D contains very sparse labelling for Cx36. (E,F) The same field (E1,E2) double labelled for vglut-1 and Cx36 in mouse hippocampal hilus, shown as a positive control for detection of Cx36-puncta in mouse hippocampus, and a similar field (F1,F2) double-labelled for vglut-1 and Cx36, showing absence of Cx36-puncta in the hilus of Cx36 knockout mice, shown as a control for anti-Cx36 specificity. Scale bars: A-D, 50 μm; E,F, 100 μm.

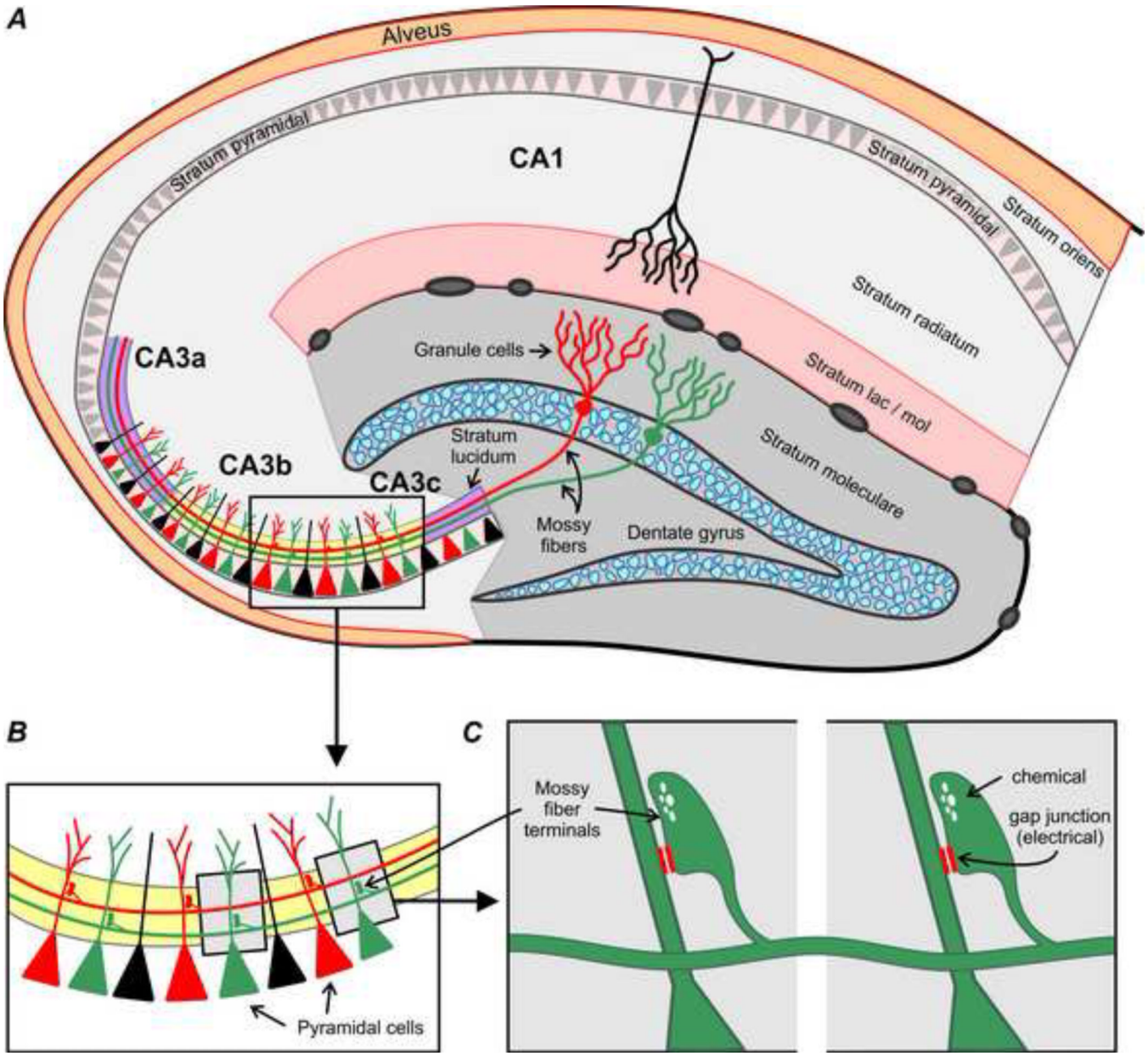

Fig. 8.

Hypothesized mechanism for mediation of electrical coupling between hippocampal CA3b and CA3c pyramidal cells via mossy fiber presynaptic axons. (A) Diagram of ventral hippocampus sectioned perpendicular to its dorsal-ventral long axis, showing the granule cell mossy fiber projection to the stratum lucidum, with mossy terminals ending on CA3b and CA3c pyramidal cells. The portion of the stratum lucidum colored yellow contains a high concentration of Cx36-puncta. (B) Magnification of box in A, showing different mossy fibers (depicted red and green) terminating in an en passant fashion on different sets of pyramidal cells (depicted red and green). (C) Magnification of boxes in B, showing a single mossy fiber terminal forming mixed chemical/electrical synapses on dendrites of two different pyramidal cells, potentially allowing the electrical component of the synapse, formed by gap junctions containing Cx36, to couple sets of pyramidal cells (two shown here) by way of the common mossy fiber axon innervating these cells. The on average eight

to fourteen pyramidal cells receiving en passant mossy terminals from a single mossy fiber are separated by greater distances (Acsady et al., 1998) than illustrated here.